EPR of radiation damage centres W11, W12, W13 and W14 in type Ib diamond

1994 J. Phys.: Condens. Matter 6 801

(http://iopscience.iop.org/0953-8984/6/3/020)

J. Phys.: Condens. Matter 6 (1994) 801–810. Printed in the UK

EPR of radiation damage centres W11, W12, W13 and W14 in type Ib diamond

J A van Wyk

Department of Physics, University of the Witwatersrand, Wits 2050, Johannesburg, South Africa

Received 3 September 1993, in final form 3 November 1993

Abstract. W11, W12, W13 and W14 are four paramagnetic defects with $S = \frac{3}{2}$ observed in electron or neutron irradiated type Ib diamonds. Although spin Hamiltonian parameters have been determined that describe the ESR results very well, it will be shown that the normal spin Hamiltonian with $S = \frac{3}{2}$ is not entirely sufficient to describe the angular dependence of the ESR spectra. Possible tentative models for the defects will be discussed.

1. Introduction

It is well known from ESR and optical studies that many defects are formed when diamonds are exposed to electron or neutron irradiation (Clark *et al* 1979, Davies 1977). The type of defect formed depends strongly on the type of diamond used. In contrast to type II diamonds, which contain little nitrogen, and type Ia diamonds, which contain clusters consisting of two or more substitutional nitrogens, type Ib diamonds contain nitrogen mainly in singly dispersed form. It is therefore expected that a particular family of radiation defects will be observed in synthetic and natural type Ib diamonds. Details about some defects observed in type IIa diamonds can be found in the article by Lomer and Welbourn (1977). In this paper we will report on four centres, referred to as W11, W12, W13 and W14, observed immediately after exposure to electron or neutron irradiation in type Ib diamonds. Very low concentrations of these centres have been observed, on occasion, in electron irradiated type Ia diamonds.

2. Experimental details

W11–W14 become detectable for electron or neutron doses around 1.0×10^{17} cm^{-2}. Measurements were generally made on diamonds that received doses between 5.0×10^{17} and 5.0×10^{18} cm^{-2}.

A Varian large-sample access cavity and 100 kHz field modulation were used in conjunction with a Varian E-line spectrometer. The cavity was mounted so that the sample could be rotated through 360° about a horizontal axis and the magnet through ±20° around a vertical axis.

0953-8984/94/030801+10$07.50

3. Angular dependence of the spectra

The ESR spectrum of W11–W14 before any annealing, and with the magnetic field applied along a ⟨111⟩ axis, is shown in figure 1. Angular dependences of the spectra in {110} planes are shown in figure 2. Initially it was difficult to identify the various lines of the spectra with each of the defects—the degree of difficulty can be visualized by imagining a superposition of these angular dependences. Fortunately the centres anneal out at different temperatures, W11 between 250 °C and 300 °C, W12 and W13 just under 400 °C and W14 just above 400 °C. Analysis of W14 became simple after the diamond was annealed at 400 °C. Although some progress was made in analysing the other defects by referring back to spectra taken after anneals at lower temperatures, final analysis was possible only after the defects were created in another type Ib diamond.

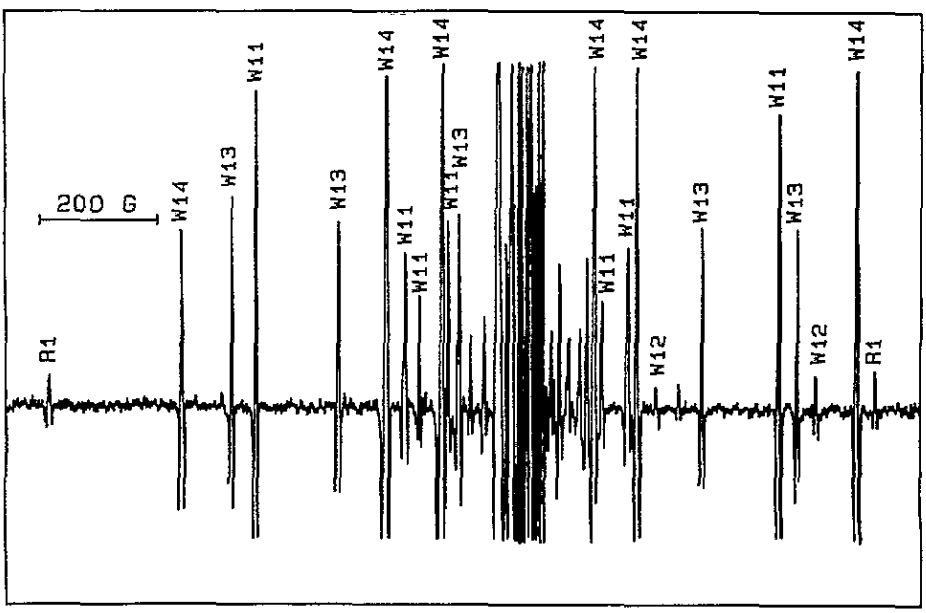

Figure 1. X band (9.0 GHz) ESR spectrum of W11, W12, W13 and W14 in an electron irradiated natural type Ib diamond with the magnetic field applied along a ⟨111⟩ axis.

Many defects in diamond have their major principal defect axis (which will be referred to as the z axis) and, for symmetries lower than axial, often another principal axis (which will be referred to as the y axis), in or close to a {110} plane. This {110} plane will be referred to as plane 1. Plane 2 is the {110} plane at right angles to plane 1; it contains the ⟨110⟩ axis at right angles to plane 1 and the principal x axis in the case of monoclinic symmetry. Planes 3 and 5 are {110} planes that share the ⟨111⟩ axis closest to the z axis with plane 1, whereas planes 4 and 6 are {110} planes sharing the ⟨111⟩ axis closest to the y axis with plane 1. With monoclinic symmetry the spectra in planes 3 and 5, and also the spectra in planes 4 and 6, will be superimposed. The angular dependences in planes 1, 2, 3 (and 5) and 4 (and 6) can be identified by circles, stars, triangles and quadrilaterals, respectively, in figure 2.

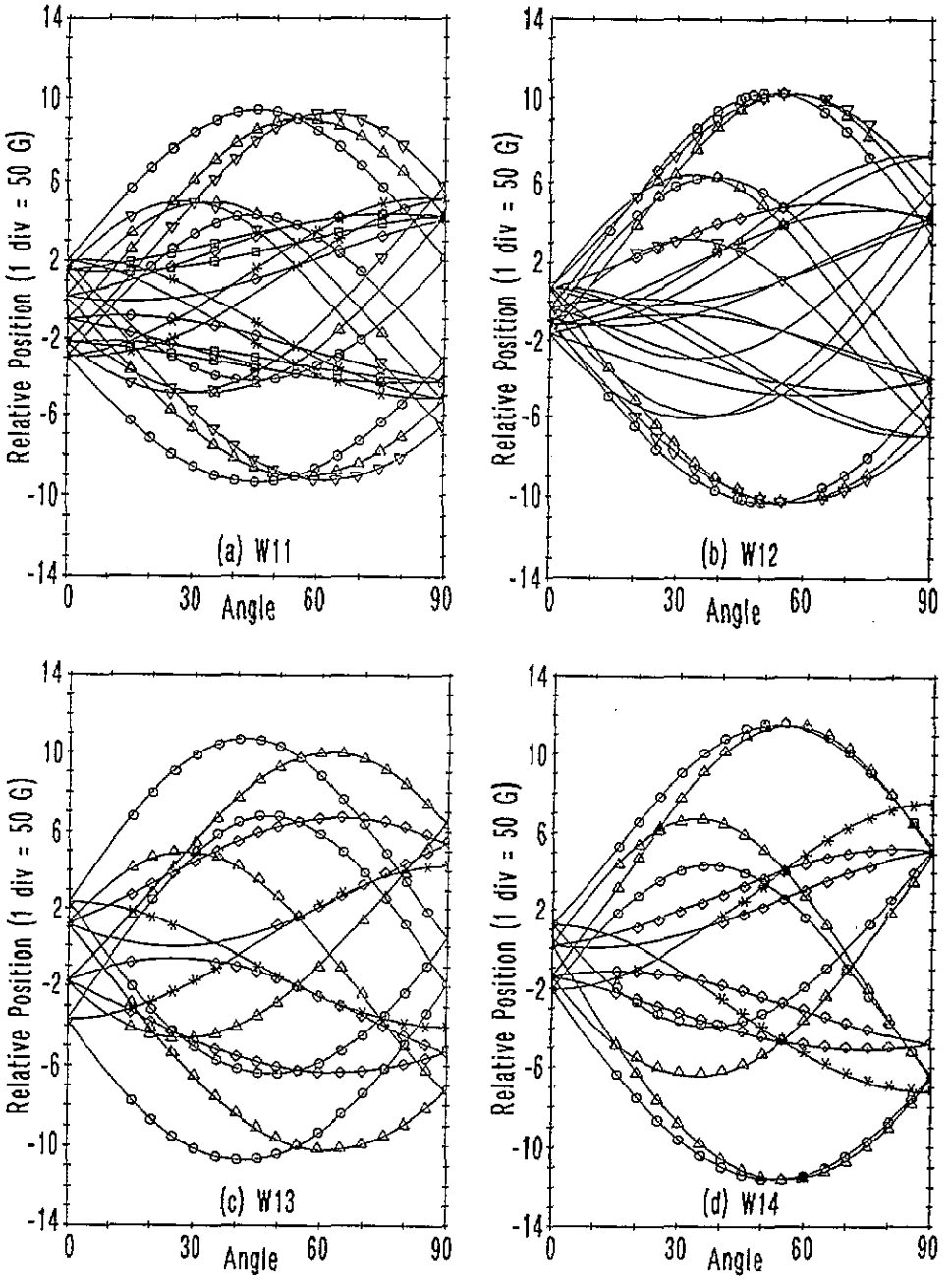

Figure 2. Angular dependence of (a) W11, (b) W12, (c) W13 and (d) W14 in the {110} planes. The circles, stars, triangles and quadrilaterals represent experimental data in planes 1, 2, 3 (and 5) and 4 (and 6), respectively (see section 3), used to determine the spin Hamiltonian parameters. The solid lines represent positions calculated using the parameters in table 1.

The angular dependences in figure 2 show then that W13 and W14 have monoclinic symmetry while W11 and W12 have triclinic symmetry.

In all samples a very strong isotropic ESR line is observed. This line has $g = 2.0029$ and shows no discernible hyperfine structure; its intensity changes as the diamond is annealed and it is probably a superposition of several resonances. Both experimental and calculated positions are plotted relative to the centre of this line. In this way the dependence of the peak positions on frequency is eliminated.

It should perhaps be noted that the intensities of W11 and W14 do not change appreciably when the diamond is rotated in the {110} planes. The intensity of W13 however is low in plane 2 and is difficult to observe when the magnetic field is applied along the x axis of the zero-field tensor. The intensities of W12 lines are generally lower than those of the other centres, and many low-field lines could not located. This explains the absence of data in the lower half of figure 2(b).

4. The spin Hamiltonian and parameters

Since most radiation defects in type IIa diamonds had $S = 1$ (Lomer and Wild 1973, Lomer and Welbourn 1977), an attempt was made to fit the spectra to the spin Hamiltonian of the form

$$\mathcal{H} = \beta \boldsymbol{H} \cdot \mathbf{g} \cdot \boldsymbol{S} + \boldsymbol{S} \cdot \mathbf{D} \cdot \boldsymbol{S}$$

where $S = 1$ and the other symbols have their usual meaning.

For the calculation of the peak position the secular equations were solved exactly using standard eigenvalue subroutines, and the spin Hamiltonian parameters were determined using normal least-squares techniques. It was found that the spectra could not be fitted satisfactorily with $S = 1$.

In these diamonds W11–W14 become detectable when, and sometimes before, R1 becomes detectable. Although R1 was troublesome in many cases it could be put to good use in finally analysing the spectra of W11–W14. First it was established by careful measurements that all lines in the spectra of R1 could be fitted to better than 1 G (the mean square deviation for 307 fields was 0.43 G) using $S = 1$. The parameters required are shown in table 1. They differ slightly from previous values (Lomer and Welbourn 1977, Lea-Wilson 1988), and the small deviation from axial symmetry for the zero-field tensor, as well as a small anisotropy for the $\mathbf{g}$ tensor, seems to be real.

Having established this, the R1 spectra were used in subsequent measurements to establish the orientation of the magnetic field, with respect to the crystal axes, to one tenth of a degree or better. In this way the possibility that disagreement between calculation and measurement were due to inaccurate angular measurements could be eliminated.

It can now be stated with confidence that parameters determined with $S = 1$ at best produce poor fits to experimental measurements.

A considerable improvement was obtained when the electron spin was changed to $S = \frac{3}{2}$. The root mean square deviation of the fit, using the same data, comes down from over 6 G to 0.4 G for W11. For the other centres the reductions in the standard deviation were even larger.

The least-squares fit parameters, with $S = \frac{3}{2}$, for all four centres are given in table 1. Also given are the root mean square deviations of the fits. Note that the fits are worse for the stabler (those that anneal out at higher temperatures) defects. The angular dependences calculated using these parameters are shown by the solid curves in figure 2.

Table 1. Spin Hamiltonian parameters for R1 and W11–W14 centres.

Parameter	R1	W11	W12	W13	W14
g_{xx}	2.0019(2)	2.0022(5)	2.0043	1.9984	1.9977
θ (°)[a]	0	isotropic	−122	0	0
ψ (°)[a]	90	isotropic	20	90	90
g_{yy}	2.0020(2)	2.0022(5)	1.9970	1.9972	1.9954
θ	−171(15)	isotropic	142	130	124
ψ	0.0	isotropic	14	0	0
g_{zz}	2.0027(2)	2.0022(5)	1.9989	2.0037	2.0037
θ	99(15)	isotropic	20	40	34
ψ	0.0	isotropic	66	0	0
D_{xx}[b]	−1408(1)	−241(3)	−143(5)	−193(3)	−346(3)
θ	0	21(5)	−51(5)	0	0
ψ	90	86(5)	58(5)	90	90
D_{yy}	−1396	−200	−338	−309	−194
θ	107.4	134	128	138.0	127
ψ	0.0	1.4	31	0.0	0.0
D_{zz}	2805(1)	441(2)	482(3)	501(2)	541(2)
θ	17.4(4)	44.5(5)	38.5(10)	48.0(5)	37.2(5)
ψ	0.0	−3.3(2)	−0.3(2)	0	0
σ[c]	0.44	0.39	2.4	2.2	3.4

[a] θ shows how much the principal axis is swung from a ⟨110⟩ axis in the {110} plane and ψ gives the tilt of the principal axes out of the [110] plane.

[b] In no case was any attempt made to determine the sign of the **D** tensor—D_{zz} were taken as positive.

[c] σ represents the square root of the mean of the sum of the squares of the residuals.

If $S = \frac{3}{2}$, then there must be $m_s = \frac{1}{2}$ to $m_s = -\frac{1}{2}$ transitions in the $g = 2$ region. It is difficult to make measurements in this region as all the centres commonly observed in unirradiated natural type Ib diamonds, viz. P1 (Smith *et al* 1959), OK1 (Klingsporn *et al* 1970, Newton and Baker 1989) N3 (Shcherbakova *et al* 1972, van Wyk *et al* 1992), the negative vacancy (Isoya *et al* 1992) and other unidentified radiation centres, do have spectra in this region. Positive identification of the $m_s = \frac{1}{2}$ to $m_s = -\frac{1}{2}$ transition for W14 was made after the diamond was annealed at 400 °C. The spectrum is shown in figure 3, and the angular dependences are shown in figure 4. Also shown in figure 4 are the calculated angular dependences (solid lines), using the parameters in table 1. On the scale of the position axis of figure 2 the fits for the outer lines appear excellent; discrepancies are however evident on scales such as those used in figure 4. There can, however, be no doubt that these lines are indeed the $m_s = \frac{1}{2}$ to $m_s = -\frac{1}{2}$ for W14. If the spectrum is observed immediately after irradiation in the $g = 2$ region, lines belonging to W13 and W14 can readily be discerned from many other lines. This is not possible for W11 and W12. The problem may be that because of the lower symmetry of these defects, and splitting of these lines into more components, these lines will be harder to detect. We will return to the broken lines in figure 4 in the following section.

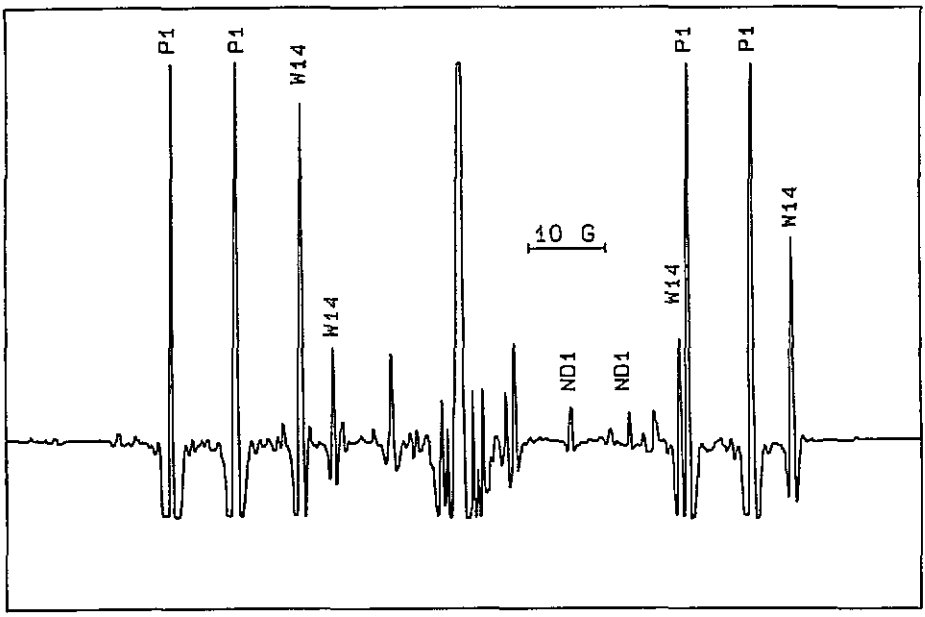

Figure 3. X-band (9.0 GHz) ESR spectrum of the $m_s = \frac{1}{2}$ to $m_s = -\frac{1}{2}$ lines of W14 in an electron irradiated natural type Ib diamond with the magnetic field applied along the ⟨110⟩ axis. The peaks labelled ND1 are due to the negative vacancy.

5. Discussion of the spin Hamiltonian parameters

Although its is reasonably certain that $S = \frac{3}{2}$ for these defects, additional evidence is provided by plotting $(H_{top} + H_{bottom})/2$. These angular dependences are determined mainly by g value variations and higher-order shifts due to the zero-field tensor. Experimental data for W11 in planes 1 and 2, as well as least squares fits using $S = 1$ and $S = \frac{3}{2}$, are shown in figure 5. W11 has been chosen to demonstrate this point as an $S = \frac{3}{2}$ Hamiltonian produced the best fit to the experimental data for this centre. It is obvious that $S = 1$ parameters do not fit the experimental data.

Although $S = \frac{3}{2}$ fits the experimental data considerably better than $S = 1$, it is not perfect. This is partly reflected by the relatively large mean square deviation of the fits for W12, W13 and W14 compared to that of R1 and W11. Comparing the calculated with the experimental data shows variations in their differences, varying with angle, and also well outside the scatter of the data. This suggests that there is still some angular dependence not accounted for, which in turn may influence the meaningfulness of some of the parameters in table 1. There is no doubt that the zero-field parameters are correct, or very nearly so. Caution should be exercised when conclusions are are drawn from the **g** tensor. The dotted lines in figure 4 were obtained with **g** parameters determined using only data for the $m_s = \frac{1}{2}$ to $m_s = -\frac{1}{2}$ lines in a least-squares fit. This fit produced an isotropic **g** tensor with $g = 2.0003(5)$. However, the anisotropic parameters in table 1 give a better fit than the isotropic parameters, for a plot of the mean fields. Until this discrepancy has been resolved one should not place too much importance on the anisotropy of the **g** tensors in table 1. For this reason no errors are quoted for the **g** tensors. The parameters as they stand can however reliably be used to calculate peak positions.

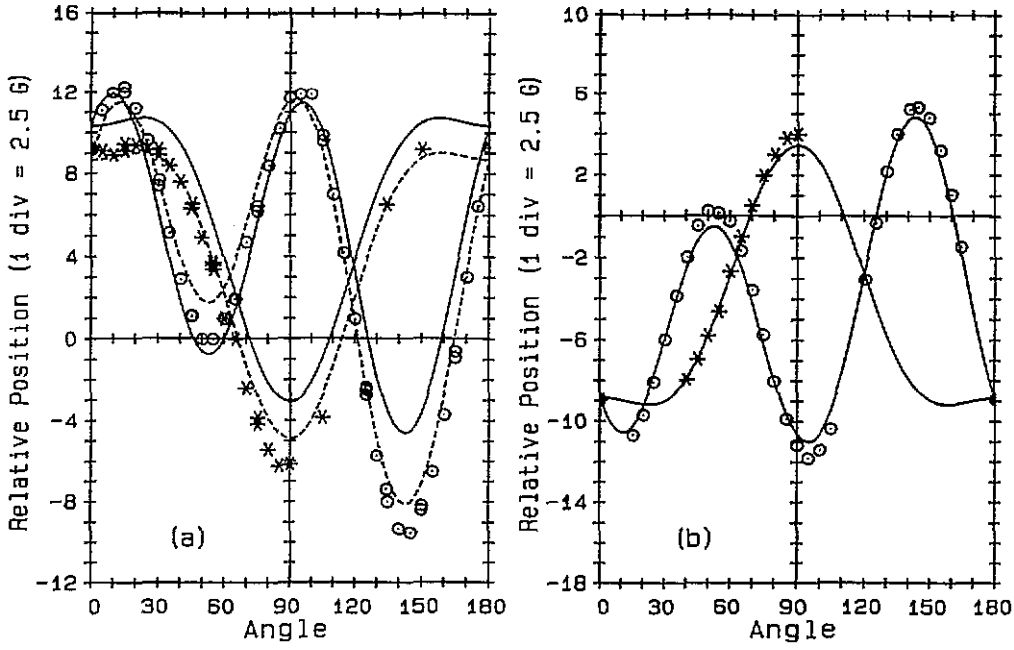

Figure 4. (a) Angular dependence of the $m_s = \frac{1}{2}$ to $m_s = -\frac{1}{2}$ lines for W14 in the {110} planes. Circles, stars, etc represent experimental data. The solid lines represent positions calculated using the parameters in table 1. The broken lines are for a **g** tensor obtained from a least-squares fit using only data for the $m_s = \frac{1}{2}$ to $m_s = -\frac{1}{2}$ transitions. (b) Angular dependence of the mean field of the $m_s = \frac{3}{2}$ to $m_s = \frac{1}{2}$ and $m_s = -\frac{3}{2}$ to $m_s = -\frac{1}{2}$ transitions. The solid lines represent mean fields calculated using the parameters in table 1.

It is clear that the spin Hamiltonian used is not entirely adequate to describe the ESR spectra. At the same time it is not obvious what the exact form, which will probably depend on the model of these defects, of the Hamiltonian should be.

6. Possible models for the centres

The following facts should be kept in mind when one tries to propose models for these defects.

(i) These centres are observed only in diamonds containing large concentrations of isolated substitutional nitrogen (P1 centres). Nitrogen should therefore be involved, directly or indirectly.

(ii) The electron spin is $\frac{3}{2}$, which means that the defects involve three unpaired electrons.

(iii) W11–W14 anneal out well below 450 °C. The model must therefore involve an entity that becomes mobile between 250 and 450 °C.

(iv) Annealing studies showed that as the less stable of these defects anneal out, increases in the concentrations of the remaining centres are observed. This possibly suggests that in the annealing process the constituents of the defects are rearranged which then leads to a conversion of one defect into another.

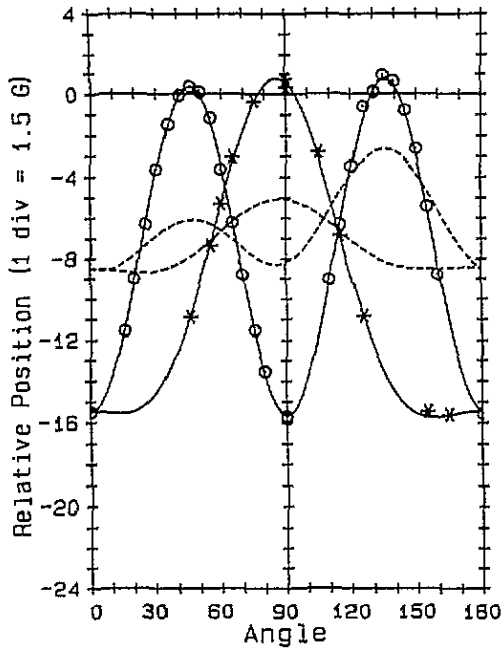

Figure 5. Angular dependence of the mean field of the $m_s = \frac{3}{2}$ to $m_s = \frac{1}{2}$ and $m_s = -\frac{3}{2}$ to $m_s = -\frac{1}{2}$ transitions, for W11. The solid line represent mean fields calculated using the parameters in table 1. The broken lines are for a least-squares fit for $S = 1$ and using the same data.

(v) In figure 1 it can be seen that the W centres are present in larger amounts than the R1 centre.

The simplest way in which three unpaired electrons can result is to assume that a vacancy traps an electron, which could come from a nearby nitrogen. Support for this approach can perhaps be found in the fact that Isoya *et al* (1992) recently showed that the negative vacancy has $S = \frac{3}{2}$. The isolated negative vacancy has T_d symmetry and no zero-field splitting is observed. It can then be proposed that if in type Ib diamonds these negative vacancies are formed close to the substitutional nitrogens, the proximity of the nitrogen will cause a lowering of the symmetry of the negative vacancy. Different positions of the nitrogen relative to the vacancy can give rise to different symmetries and zero-field splittings. On this basis one might have expected to observe a comparable concentration of nitrogen–vacancy pairs in nearest-neighbour positions relative to each other. Such a defect should have had trigonal symmetry around ⟨111⟩ axes. No evidence for a defect like this, with $S = \frac{3}{2}$, has been observed. Small amounts of the W15 centre (Loubser and van Wyk 1977, He *et al* 1993), which has trigonal symmetry around ⟨111⟩ axes, and which is believed to be due to nearest-neighbour vacancy–nitrogen pairs, are sometimes observed after irradiation. However, the spin of this defect is definitely 1, showing that it involves an even number of electrons, and it becomes prominent only when the vacancies become mobile around 700 °C. Also, if these defects only consist of a vacancy and substitutional nitrogen, it will be difficult to understand the interconversion and annealing out of these defects at temperatures below 450 °C, unless the mobility of either the vacancy or the substitutional nitrogen is enhanced in the vicinity of the other at these temperatures.

A second possibility could be that one or more interstitial atoms are trapped at different positions near a negative vacancy. At this moment it is not clear how such a vacancy–interstitial(s) cluster can be stable. Also, readily detectable amounts of isolated negative vacancies are observed in type Ia diamonds. If the negative vacancy traps either carbon or nitrogen interstitials to form W11–W14, one might have expected to observe these defects in type Ia diamonds. It was pointed out that very small amounts (if any) of W11–W14 are observed in these diamonds.

Another possibility is the following. The valence electrons of both nitrogen and carbon are accommodated in 2p states, and a $2p^3$ configuration would give rise to a ^4S state, which has $S = \frac{3}{2}$. Neutral interstitial nitrogen already has the correct electron configuration, but the absence of hyperfine interactions, and other considerations, rules this possibility out. Let us now consider interstitial C^- ions. The fact that the W centres are observed in both natural and synthetic type Ib diamonds indicates that the formation of the defects depends crucially on the presence of P1 centres, and not on the presence of other nitrogen defects or other impurities. Is it not possible now to form an ionically bonded $P1^+$–C^- pair by the transfer of the fifth nitrogen electron to an interstitial carbon? The paramagnetism of the defect will then be associated with the interstitial carbon, which does have the correct electron spin, and which can be delocated easily to account for its annealing behaviour. However, this requires that four different sites for the trapping of the carbon must be available near the nitrogen in order to account for the observation of the four different centres. At the moment it is not clear why there should be specifically four sites. There is always the possibility that vacancies or other radiation products may also be involved, but this will necessarily lead to complications and the number of possible combinations may then be larger than the small number of four observed.

It is evident that the last word has not been said on these defects and more experimental and theoretical work will have to be done to determine the final models for them.

Acknowledgments

The author would like to thank the management of the Diamond Research Laboratory of De Beers Industrial Division for providing the diamonds required in this work. We would also like to thank Diamond Research Laboratories and the Condensed Matter Research Unit for their financial support.

References

Clark C D, Mitchell E W J and Parsons 1979 *The Properties of Diamond* ed J E Field (London: Academic) pp 23–77

Davies G 1977 *Chem. Phys. Carbon* **13** 1

He X, Manson N B and Fisk P T H 1993 *Phys. Rev.* B **47** 8809–22

Isoya J, Kanda H, Uchida Y, Lawson S C, Yamasaki S, Itoh H and Morita Y 1992 *Phys. Rev.* B **45** 1436–9

Klingsporn P E, Bell M D and Leivo W J 1970 *J. Appl. Phys.* **41** 2977–80

Lea-Wilson M A 1988 *PhD Thesis* Reading University

Lomer J N and Welbourn C M 1977 *Radiation Effects in Semiconductors 1976 (Inst. Phys. Conf. Ser. 31)* (Bristol: Institute of Physics) pp 339–45

Lomer J N and Wild A M A 1973 *Radiat. Effects* **17** 37–44

Loubser J H N and van Wyk J A 1977 *Diamond Res. (Suppl. to Ind. Diamond Rev.)* 11–14

Newton M E and Baker J M 1989 *J. Phys.: Condens. Matter* **1** 10549–61

Shcherbakova M Ya, Sobolev E V and Nadolinnyi V A 1972 *Sov. Phys.–Dokl.* **17** 513–16
Smith W V, Sorokin P P, Gelles I L and Lasher G J 1959 *Phys. Rev.* **115** 1546–52
van Wyk J A, Loubser J H N, Newton M E and Baker J M 1992 *J. Phys.: Condens. Matter* **4** 2651–62